



19 Obesity, a risk factor for the development of type-2 diabetes, hypertension, cardiovascular  
20 disease, hepatic steatosis and some cancers, has been ranked in the top 10 health risk in the  
21 world by the World Health Organization. Despite the growing body of literature evidencing  
22 an association between the obesity epidemic and specific chemical exposure across a wide  
23 range of animal taxa, very few studies assessed the effects of chemical mixtures and  
24 environmental samples on lipid homeostasis. Additionally, the mode of action of several  
25 chemicals reported to alter lipid homeostasis is still poorly understood. Aiming to fill some  
26 of these gaps, we combined an *in vivo* assay with the model species zebrafish (*Danio rerio*)  
27 to screen lipid accumulation and evaluate expression changes of key genes involved in lipid  
28 homeostasis, alongside with an *in vitro* transactivation assay using human and zebrafish  
29 nuclear receptors, retinoid X receptor  $\alpha$  and peroxisome proliferator-activated receptor  $\gamma$ .  
30 Zebrafish larvae were exposed from 4 day post-fertilization until the end of the experiment  
31 (day 18), to six different treatments: experimental control, solvent control, tributyltin at 100  
32 ng/L Sn and 200 ng/L Sn (positive control), and wastewater treatment plant influent at  
33 1.25% and 2.5%. Exposure to tributyltin and to 2.5% influent led to a significant  
34 accumulation of lipids, with white adipose tissue deposits concentrating in the perivisceral  
35 area. The highest *in vitro* tested influent concentration (10%) was able to significantly  
36 transactivate the human heterodimer PPAR $\gamma$ /RXR $\alpha$ , thus suggesting the presence in the  
37 influent of HsPPAR $\gamma$ /RXR $\alpha$  agonists.  
38 Our results demonstrate, for the first time, the ability of complex environmental samples  
39 from a municipal waste water treatment plant influent to induce lipid accumulation in  
40 zebrafish larvae.

41 *Keywords: obesity, obesogen, endocrine disruptor, environmental mixture, nuclear*  
42 *receptor.*

## 43 **1. INTRODUCTION**

44 Obesity, the result of a prolonged disturbance of energy homeostasis favoring triglyceride  
45 storage and adipocyte hypertrophy, has been reported to be reaching epidemic proportions,  
46 affecting developed and developing countries and increasing prevalence among children  
47 and animals (Chamorro-García and Blumberg, 2014; Grün and Blumberg, 2009; Landgraf  
48 *et al.*, 2017; Newbold *et al.*, 2007; Minchin & Rawls, 2011; Santos *et al.*, 2012). In addition  
49 of being a risk factor for type-2 diabetes, hypertension, cardiovascular disease, hepatic  
50 steatosis, premature mortality and some cancers, among other medical conditions (Grün and  
51 Blumberg, 2009; Landgraf *et al.*, 2017; Minchin and Rawls, 2011; Newbold *et al.*, 2007),  
52 obesity has a detrimental impact on economic development costing billions of dollars  
53 annually in direct or indirect care (Spencer & Tilbrook, 2011). Consequently, it is ranked in  
54 the top 10 health risks in the world by the World Health Organization, with the number of  
55 overweight people exceeding the number of undernourished ones worldwide (Newbold *et*  
56 *al.*, 2007).

57 An increasing body of evidence suggest that this condition does not develop solely from a  
58 chronic positive energy balance (high caloric intake *versus* lack of exercise), but is rather a  
59 consequence of complex interactions between genetic and environmental factors (Bašić *et*  
60 *al.*, 2012; Capitão *et al.*, 2017; Chamorro-García and Blumberg, 2014; Dimastrogiovanni *et*  
61 *al.*, 2015; Grün and Blumberg, 2009; Lyssimachou *et al.*, 2015; Minchin and Rawls, 2011;  
62 Newbold *et al.*, 2007; Santos *et al.*, 2012; Spencer and Tilbrook, 2011). The disruption of  
63 energy homeostasis by endocrine disrupting chemicals (EDCs) is an emerging new field  
64 and could explain the rapid increase in obesity rates observed in animals living in close  
65 proximity to human populations in industrialized societies (Chamorro-García and  
66 Blumberg, 2014; Grün and Blumberg, 2009; Klimentidis *et al.*, 2011; Lyssimachou *et al.*,  
67 2015; Newbold *et al.*, 2007), which coincided with the massive release of industrial  
68 chemicals over the past decades (Newbold *et al.*, 2007; Santos *et al.*, 2012).

69 Lipid homeostasis is controlled by complex networks and feedback mechanisms involving  
70 several body organs, transcription factors (e.g. nuclear receptors (NR)), enzymes, hormones  
71 and nutrients, with a complex cross-talk between different signaling pathways (Capitão *et*  
72 *al.*, 2017, 2018; Moseti *et al.*, 2016). The central nervous system is the coordinator of all  
73 these processes, acting as a lipid and hormone sensor and integrating and transforming  
74 afferent information from other organs into signals that will ensure necessary adjustments,  
75 for example, by changing feeding behavior or energy expenditure (Lyssimachou *et al.*,  
76 2015; Santos *et al.*, 2012). The adipose tissue, besides being one of the main tissues for the  
77 occurrence of lipogenesis and where the excess of fatty acids are stored in the form of  
78 triglycerides (Kersten, 2001; Lyssimachou *et al.*, 2015; Moseti *et al.*, 2016; Santos *et al.*,  
79 2012), functions also as an endocrine and immune organ (Bašić *et al.*, 2012; Birsoy *et al.*,  
80 2013; Santos *et al.*, 2012).

81 Members of the peroxisome proliferator-activated receptors (PPARs), transcription factors  
82 from the NR superfamily play essential roles in adipocyte differentiation and energy  
83 homeostasis, forming obligate heterodimers with the retinoid X receptor (RXR) which  
84 changes the transcription of target genes upon the binding of a ligand to the ligand binding  
85 domain (LBD) (Janesick and Blumberg, 2011; Santos *et al.*, 2018, 2012; Yoon, 2009). Each  
86 subtype possesses different ligand specificity, tissue distributions and biological functions  
87 (Santos *et al.*, 2012; Yoon, 2009).

88 Widely known as the “Master regulator of adipogenesis”, due to its absolute requirement  
89 for the process, PPAR $\gamma$  is mostly expressed in adipocytes and directly induces genes that  
90 regulate the adipogenic cascade, glucose uptake, lipid uptake, synthesis and storage (Birsoy  
91 *et al.*, 2013; Janesick and Blumberg, 2011; Lyssimachou *et al.*, 2015; Moseti *et al.*, 2016;  
92 Santos *et al.*, 2012). As its ligand-binding pocket is large enough to accept a variety of  
93 chemical structures, this NR is particularly sensitive to environmental chemicals (Capitão *et*  
94 *al.*, 2018; Janesick and Blumberg, 2011; Lyssimachou *et al.*, 2015) and since the

95 RXR:PPAR $\gamma$  heterodimer is permissive, either receptor pocket can be targeted by ligands  
96 and mediate its signaling (Grün & Blumberg, 2009). Moreover, PPARs occur in vertebrate  
97 and some non-vertebrate groups (Cephalochordates, Urochordates, Molluscs and  
98 Echinoderms) and RXRs in most metazoans, indicating a wide taxonomic scope of the  
99 inappropriate regulation of these pathways (Lyssimachou *et al.*, 2015; Santos *et al.*, 2012).  
100 Moreover, RXR is the heterodimeric partner of several other nuclear receptors that are  
101 involved in lipid homeostasis to some extent [e.g. Liver X Receptor (LXR) and Farnesoid X  
102 Receptor] and also form permissive heterodimers (Capitão *et al.*, 2017).

103 Obesogens are a class of EDCs capable of interfering with the lipid metabolic pathways  
104 either directly, through interaction with NR leading to changes in patterns of gene  
105 expression stimulating adipogenesis and fat accumulation, or indirectly by mimicking or  
106 blocking the action of natural hormones and regulating appetite and satiety (Grün and  
107 Blumberg, 2007; Janesick and Blumberg, 2011; Lyssimachou *et al.*, 2015; Newbold *et al.*,  
108 2007). Yet, several other chemicals may affect lipid homeostasis through mechanisms that  
109 do not lead to lipid accumulation (Coimbra *et al.* 2015; Capitão *et al.*, 2017). Natural or  
110 xenobiotics, these chemicals are widely used in everyday products (e.g. food packages,  
111 medical devices, toys, cosmetics) (Janesick & Blumberg, 2011), from which they might  
112 leach promoting their ubiquitous presence in the environment and threatening not only  
113 human populations worldwide, but also the ecosystems (Capitão *et al.*, 2017).

114 The exact MoA of some of these chemicals has not yet been determined, as they may act on  
115 the several distinct levels aforementioned. Exposure to lipid homeostasis regulators *in utero*  
116 and during early development can alter developmental programming leading to obesity later  
117 in life (Bašić *et al.*, 2012; Grün and Blumberg, 2007; Newbold *et al.*, 2007; Santos *et al.*,  
118 2012), as evidenced by mesenchymal stem cells (MSC) with fates biased towards the  
119 adipogenic lineage following exposure (Chamorro-Garcia & Blumberg, 2014). Other  
120 possible MoA include epigenetic modifications which could modify the expression of genes

121 (Bašić *et al.*, 2012; Chamorro-Garcia & Blumberg, 2014; Newbold *et al.*, 2007) and lead to  
122 an obesogenic effect at a transgenerational level (Chamorro-Garcia *et al.*, 2017; Chamorro-  
123 García and Blumberg, 2014). Post-translational modifications, reported to occur in several  
124 enzymes and transcription factors involved in lipid metabolism (Carnitine  
125 palmitoyltransferase I (Guan *et al.* 2016), ACC (Capitão *et al.*, 2017; Wang *et al.*, 2015),  
126 PPAR $\gamma$  (van Beekum *et al.*, 2009), SREBP (Wang and Sul, 2013)), could affect the  
127 interactions of NRs with the transcriptional machinery and the processing, activity, stability  
128 and degradations of proteins, as well as their affinity for certain substrates (Guan *et al.*,  
129 2016; Janesick and Blumberg, 2011; Lempradl *et al.*, 2015; Wang and Sul, 2013). In  
130 addition to the conformational change in the receptors and induction of transcriptional  
131 activation through the binding of a ligand, nuclear receptors can also be activated or  
132 unrepressed through these post-translational modifications in the absence of ligands  
133 (Janesick & Blumberg, 2011).

134 Amongst the 1300 chemicals identified as potential EDCs, very few have been evaluated  
135 through lipid homeostasis disruption endpoints (Capitão *et al.*, 2017). So far, identified  
136 obesogens include members of the organotins, thiazolidinediones, phthalates, bisphenol-A  
137 and its polybrominated and polychlorinated derivatives, organochlorine pesticides,  
138 organophosphates, carbamates, solvents and heavy metals such as cadmium and lead, as  
139 well as estrogenic chemicals and phytoestrogens (Biemann *et al.*, 2014; Grün and  
140 Blumberg, 2007; Janer *et al.*, 2007; Janesick and Blumberg, 2011; Jordão *et al.*, 2015, 2016  
141 Newbold *et al.*, 2007; Riu *et al.*, 2014, 2011; Santos *et al.*, 2012; Watt and Schlezinger,  
142 2015), but in addition to the lack of information regarding their MoA, data concerning their  
143 interactions in mixtures, as they are found in the environment, is scarce (Biemann *et al.*  
144 2014; Capitão *et al.*, 2017).

145 The overall aim of this study was to evaluate the effects of complex environmental samples  
146 from a waste water treatment plant (WWTP) on lipid accumulation in zebrafish larvae. As a

147 proxy to better understand the underlying MoA of this complex samples, primary  
148 approaches were also conducted using transactivation assays with PPAR $\gamma$ /RXR $\alpha$ , alongside  
149 with the determination of expression of key lipogenic and adipogenic genes in zebrafish  
150 larvae.

## 151 2. METHODOLOGY

### 152 2.1. *In vivo* assay

#### 153 2.1.1. Species selection

154 The zebrafish (*Danio rerio*), a freshwater cyprinid in the Actinopterygii class, is an  
155 emerging model for the study of lipid metabolism and metabolic diseases (Hölttä-Vuori *et*  
156 *al.*, 2010; Landgraf *et al.*, 2017). Besides the widely known advantages of this species (e.g.  
157 small size, known ideal growth conditions, large number of eggs, short life cycle), it shows  
158 a high conservation of genes, NRs and molecular processes regulating energy homeostasis  
159 between mammals and teleosts and the ability to develop metabolic diseases also reported  
160 in humans (e.g. hepatic steatosis) (Birsoy *et al.*, 2013; Hill *et al.*, 2005; Hölttä-Vuori *et al.*,  
161 2010; Landgraf *et al.*, 2017; Lyssimachou *et al.*, 2015). Studying altered gene expression in  
162 response to toxic insults by real-time PCR (qPCR) or genomic screens is facilitated since  
163 the zebrafish genome is completely sequenced (Hill *et al.*, 2005; Veldman and Lin, 2008).  
164 Another advantage is its optical clarity which allows the screening of lipid accumulations  
165 using staining techniques with fluorescent dyes in small larvae without dissecting them.

#### 166 2.1.2. Animal breeding

167 All experiments with living fish were conducted in the facilities of BOGA (Biotério dos  
168 Organismos Aquáticos – CIIMAR) and have been approved by the CIIMAR ethical  
169 committee and by CIIMAR Managing Animal Welfare Body (ORBEA) according to the  
170 European Union Directive 2010/63/EU.

171 A breeding stock of adult wild-type zebrafish (*Danio rerio*; Singapore) was kept in a 250L  
172 aquarium with dechlorinated aerated water ( $28 \pm 1^\circ\text{C}$ ), under a photoperiod of 14:10h  
173 (light:dark). The fish were fed with commercial diet Tetramin (Tetra, Germany) twice a  
174 day. Nine females and nine males were placed in cages within a 30L aquarium, the cages  
175 possessing a net bottom covered with glass marbles, preventing eggs from being consumed  
176 by adults.

177 In the following morning, fertilized eggs were collected, cleaned and randomly allocated to  
178 different experimental aquaria.

### 179 2.1.3. Test conditions

180 The embryos obtained by natural mating were raised in 3L aquaria with dechlorinated water  
181 ( $28 \pm 1^\circ\text{C}$ ) with a 14L:10D photoperiod. Each aquarium contained 80 eggs.

182 From hatching, 4th day post-fertilization (dpf) until the end of the experiment (18<sup>th</sup> dpf), the  
183 larvae were exposed to six different treatments in duplicate: experimental control, solvent  
184 control (0.0002% dimethylsulfoxide, DMSO), tributyltin (TBT) at 100 ng/L Sn and 200  
185 ng/L Sn (positive control), and wastewater treatment plant influent at 1.25% and 2.5%. TBT  
186 was selected as a positive control given that Lyssimachou et al., (2015) previously  
187 demonstrated massive fat accumulation in zebrafish following a life-cycle exposure to  
188 environmentally relevant concentrations. TBT test solutions were obtained by successive  
189 dilutions of a stock solution containing TBT chloride (96%, Sigma-Aldrich) in DMSO  
190 (99.9%, Sigma-Aldrich). All aquaria had the same DMSO concentration with exception of  
191 experimental control. The 24-h composite WWTP influent was obtained at the Porto  
192 municipal waste water treatment plant facility in 2017, between 3 and 9 of May,  
193 encompassing a full week from Wednesday to Tuesday. Samples were collected daily for  
194 seven consecutive days, frozen immediately after collection to prevent degradation of the  
195 compounds and used within 1 month for the assays, following a similar sampling design of

196 that described by González-Mariño *et al.*, (2017) and Gracia-Lor *et al.*, (2017). This WWTP  
197 serves a population of approximately 150.000 people (mean flux of 33000 m<sup>3</sup>/day)  
198 (González-Mariño *et al.*, 2017; Gracia-Lor *et al.*, 2017). The samples were characterized  
199 upon collection (mean pH= 7,03; T= 21°C; Ammonium (mg/L) 47,8). A preliminary  
200 characterization of the composite influent was performed by Liquid Chromatography  
201 Quadrupole Time-of-flight Tandem Mass Spectrometry (LC-QTOF-MS/MS) with a  
202 particular focus on putative PPAR/RXR agonists as detailed in the Supporting Information  
203 Table S1 (**Appendix A**). Detected compounds were classified in confirmatory levels as  
204 proposed by (Schymanski *et al.*, 2014).

205 The medium was renewed daily, ammonia levels checked weekly using Palintest tablets and  
206 Palintest Photometer 7000se ( $0.3625 \pm 0.033$  mg/L N and  $0.4375 \pm 0.0369$  mg/L N for the  
207 1.25% and 2.5% WWTP influent, respectively, and  $0.1425 \pm 0.0347$  mg/L N for all  
208 remaining treatments), while the temperature was monitored daily. Values of mortality were  
209 registered daily and the dead larvae/eggs were removed. Total mortality did not differ  
210 among groups (data not shown) and was maintained below 20% up to the end of the assays,  
211 which is within the normal range of the species in laboratory assays (Coimbra *et al.*, 2015).  
212 A light aeration was introduced to the aquaria on the 11th dpf.

213 Throughout the whole experiment, care was taken in order to avoid the suffering and  
214 distress of the animals.

#### 215 2.1.4. Feeding protocol

216 From 5 to 14 dpf larvae were fed with a standard diet (SD), Gemma Micro (Skretting),  
217 supplemented with cod liver oil (Fagron) to obtain a final lipid content of 25% dry matter.  
218 *Artemia spp.* cysts (Brine Shrimp Eggs; Ocean Nutrition) put to hatch for 16 hours were  
219 supplied every other day from 7 to 13 dpf (0.2 grams fed 3 aquaria). From the 15<sup>th</sup> to the  
220 16<sup>th</sup> dpf, larvae were fed lyophilized chicken egg yolk as a high fat diet (HFD), followed by

221 one day of starvation prior to the analysis on the 18<sup>th</sup> dpf. The specifications of the feeding  
 222 regime are summarized in **table 1**.

223 **Table 1.** Feeding regime throughout the assay.

	Period (dpf)				
	0 to 4	5 to 11	12 to 14	15 to 16	17 to 18
Feeding type	Not fed	Gemma Micro 100- 200 µm	Gemma 100-200 and 200-400 µm	Lyophilized egg yolk; Gemma 200-400 µm	Fasting state
Quantities	None	12 mg x3	24 mg (100- 200 µm x2; 200-400 µm x1)	egg yolk 40 mg x1; Gemma 24 mg x2	None

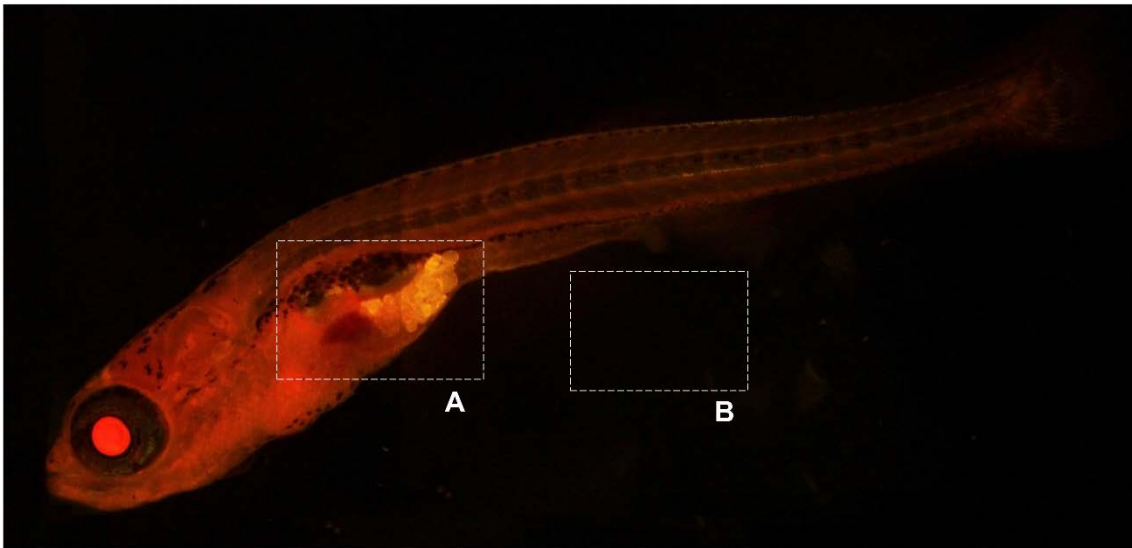
224

225 2.1.5. Nile Red staining

226 On the 18<sup>th</sup> dpf, 7 larvae of similar size ( $6.55 \pm 0.56$  mm) were selected per aquarium  
 227 and individually incubated with Nile Red (Sigma-Aldrich) (stock of 5 mg/mL in acetone  
 228 diluted 1:1000 in dechlorinated water) in 3mL-wells plates, for 60 minutes, at 28 °C in the  
 229 dark. The larvae were rinsed twice with dechlorinated water and anesthetized during 30  
 230 seconds with Tricaine 1000mg/g (Pharmaq) (stock of 168 mg/mL diluted 1:1000 in  
 231 dechlorinated water).

232 The larvae were analyzed in water within approximately 2 minutes, under the  
 233 microscope Nikon Eclipse TS100 with fluorescence filter B-2A: EX: 450-490nm, BA:  
 234 520nm. All images were captured under the same settings with imaging software NIS-  
 235 Elements D (version 4.13). Fluorescence signals were determined using ImageJ software

236 (National Institutes of Health), by converting the images into 8-bit grayscale, measuring  
237 the background fluorescence, and subtracting to the value of larvae fluorescence obtained  
238 by selecting the white adipose tissue (WAT) and individual adipocytes in the perivisceral  
239 area (**Figure 1**).



240

241 **Figure 1. Zebrafish at the 18<sup>th</sup> dpf colored with Nile Red dye; A: Perivisceral area**  
242 **containing the analyzed WAT and individual adipocytes; B: Example of area for**  
243 **background fluorescence (note: image not converted to 8-bit grayscale).**

244 The remaining zebrafish were euthanized in Ethyl 3-aminobenzoate methanesulfonate  
245 (98%; Sigma-Aldrich) at 200 mg/L to guarantee minimum pain and alleviation from  
246 discomfort, according to Annex IV of the EU Directive 2010/63/EU, and were stored in  
247 RNAlater (Sigma) for posterior molecular biology determinations.

248 2.2. Gene expression

249 2.2.1. RNA extraction and cDNA synthesis

250 The RNA extraction was performed for each body of larvae using illustra<sup>TM</sup> RNA spin Mini  
251 RNA Isolation kit (GE Healthcare) and the RNA quality was confirmed with 1% agarose

252 gel. The concentration of total RNA was determined using Gen5™ software and equipment  
253 Synergy HT Multi-Mode Plate Reader (BioTek).

254 Total cDNA was synthesized from 200 ng of RNA using the iScript™ cDNA Synthesis  
255 (Bio-Rad) kit and TGradient Thermocycler (Biometra). All assays were performed by  
256 following the kits' protocols.

#### 257 2.2.2. Real-time PCR

258 The expression of reference gene  $\beta$ -actin and target genes PPAR $\gamma$ , RXR $\alpha$ , FASn, ACOX,  
259 SREBP1, CCAAT/enhancer-binding protein  $\alpha$  (C/EBP $\alpha$ ) and diacylglycerol acyltransferase  
260 (DGAT2), individually, was assessed for each body of larvae separately, using Mastercycler  
261 ep realplex system (Eppendorf). Primers (**Table S2**) were designed with Primer-Blast-NCBI  
262 tool and synthesized by STABVIDA (Portugal).

263 Each sample was amplified in duplicate, loaded into 96-well PCR plates containing 10  $\mu$ L  
264 of reaction volume corresponding to 1  $\mu$ L of cDNA (equals 10 ng), 5  $\mu$ L of IQ™ SYBR®  
265 Green Supermix (Bio-Rad) and 200 nM of each primer.

266 The two-step qPCR program was performed according to the Taq polymerase's protocol,  
267 with a melting curve (55-95°C with 0.5°C increment) being generated at the end to confirm  
268 the specificity of each amplification. Products were also visualized through agarose gel  
269 electrophoresis, confirming the presence of single bands. The specificity of the  
270 amplification was verified by adding a "no template control" to each plate and the  
271 efficiency determined for each gene through standard curves with successive dilutions of  
272 cDNA pools from each sample (6 dilution steps with dilution factor 1:5). Efficiencies  
273 between 88-109% were considered acceptable. The reference gene was validated by its  
274 stability among the exposure groups and controls, verified through one-way ANOVA.

275 The relative quantification of target genes was performed according to Livak's method  
276 (Livak & Schmittgen, 2001). Relative changes in gene expression were calculated based on  
277 the amount of target normalized to  $\beta$ -actin and relative to an internal calibrator:

$$278 \text{ Amount of target} = 2^{-\Delta\Delta Ct} = (2^{-(Ct_{\text{sample}} - Ct_{\text{calibrator}})_{\text{target}}}) / (2^{-(Ct_{\text{sample}} - Ct_{\text{calibrator}})_{\text{reference}}})$$

### 279 2.3. Transactivation assays

#### 280 2.3.1. Plasmid constructs

281 Primers were designed using Primer 3 to amplify the Hinge Region (HR) plus LBD of  
282 human and zebrafish RXR $\alpha$  and PPAR $\gamma$  (**Table S3**), with insertion of additional  
283 oligonucleotides of recognition sequences for restriction enzymes XbaI and KpnI  
284 (Promega).

285 A rapid amplification of cDNA ends PCR was performed using zebrafish cDNA pool as a  
286 template for RXR $\alpha$  and zebrafish liver cDNA for PPAR $\gamma$ . The products were gel-purified  
287 and digested with restriction enzymes, for insertion of RXR $\alpha$  and PPAR $\gamma$  in pBIND vectors  
288 and insertion of RXR $\alpha$  in a pACT vector. Constructs' integrity and correct orientation of  
289 inserts were verified through Sanger sequencing.

#### 290 2.3.2. Transactivation assay

291 The characterization of RXR $\alpha$ , PPAR $\gamma$  and heterodimer responses to different compounds  
292 was attained using the CheckMate™ Mammalian Two-Hybrid System (Promega). Viable  
293 COS-1 cells (kidney, *Chlorocebus sabaues*), distributed at a density of  $2 \times 10^5$  cells/mL were  
294 grown in DMEM with phenol red (PANBiotech), supplemented with 1%  
295 Penicillin/Streptomycin (PANBiotech) and 10% fetal bovine serum (PANBiotech) for 24h  
296 at 37 °C and 5% CO<sub>2</sub>. The plasmids were transfected into the cells (confluence around  
297 80%), using lipofectamine (Invitrogen), Opti-MEM 1x (Gibco), 500 ng of pBind and pGL4,  
298 as well as 750 ng of pcDNA3 (or pACT for heterodimer assays) and incubated for 5 hours

299 (André *et al.*, 2017). Zebrafish and human NRs were exposed to the treatments for 24h:  
300 DMEM without phenol-red supplemented with 1% Penicillin/Streptomycin and 10%  
301 charcoal-treated Fetal Bovine Serum (PANBiotech) was contaminated with DMSO 0.1%  
302 (solvent control; 99.9%, Sigma-Aldrich), TBT 250 nM (positive control; TBT chloride  
303 96%, Sigma-Aldrich) and 3 dilutions of WWTP influent (1.25%, 2.5%, 10%).

304 On the following day, cells were lysed with 1x Passive Lysis Buffer (Promega) and the  
305 luciferase activity was detected using the Dual-Luciferase® Reporter Assay System  
306 (Promega). The luminescence was measured using equipment Synergy HT Multi-Mode  
307 Plate Reader (BioTek), with Gen5™ software. Three replicates were performed for each  
308 transactivation assay.

#### 309 2.4. Statistical analysis

310 The statistical analysis was performed on IBM SPSS Statistics 24 software, where the  
311 homogeneity of variance of all data was confirmed using Levene's tests, prior to analysis  
312 through one-way ANOVA.

313 The Nile-Red fluorescence data, real-time PCR results and transactivation results were  
314 further analyzed through Fisher's Least Significant Difference (LSD) post-hoc test.

315 When parametric assumptions were not attained, even after square-rooting or log-  
316 transforming the data, the results were analyzed using non-parametric Mann-Whitney *U*  
317 test.

318 In all cases, *p*-values lower or equal to 0.05 were considered statistically significant.

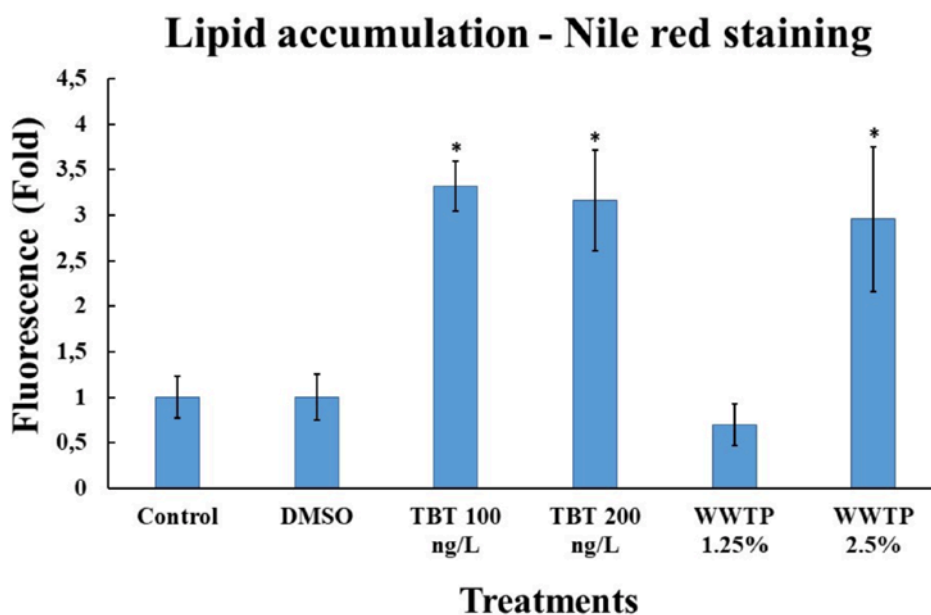
### 319 **3. RESULTS AND DISCUSSION**

#### 320 3.1. Lipid accumulation

321 Despite the conservation of several signaling pathways regulating lipid homeostasis  
322 throughout metazoans, the majority of studies on the effects of obesogens has focused on

323 mammalian models (Capitão *et al.*, 2017). Hence for a better understanding of effects and  
324 possible MoA of chemicals impacting lipid homeostasis across vertebrates, this study  
325 combines *in vivo* assays alongside with molecular and biochemical techniques using the  
326 vertebrate model species *Danio rerio*. The study aimed to address two key questions: are  
327 complex environmental samples from WWTP able to induce an obesogenic response in  
328 zebrafish larvae? If so, and as a proxy to better understand the underlying molecular mode  
329 of action, does it involve the modulation of RXR $\alpha$ /PPAR $\gamma$  signaling pathways?

330 **Figure 2** displays the results from the *in vivo* assay presenting the lipid accumulation,  
331 analyzed through Nile-red staining. Obtained values correspond to the Integrated Density  
332 (the product of area and mean gray value), representing the fluorescence captured for each  
333 larva on ImageJ Software (Figure 1). Higher values indicate greater accumulation of lipids.  
334



335

336 **Figure 2. *In vivo* induction of lipid accumulation analyzed by Nile Red staining after**  
337 **exposure to TBT and WWTP influents. TBT and WWTP influent values were expressed**

338 as average fold changes  $\pm$  SEM (N=7) of the solvent control and experimental control  
339 groups, respectively. \* $p < 0.05$  (one-way ANOVA, followed by Fisher LSD's test).

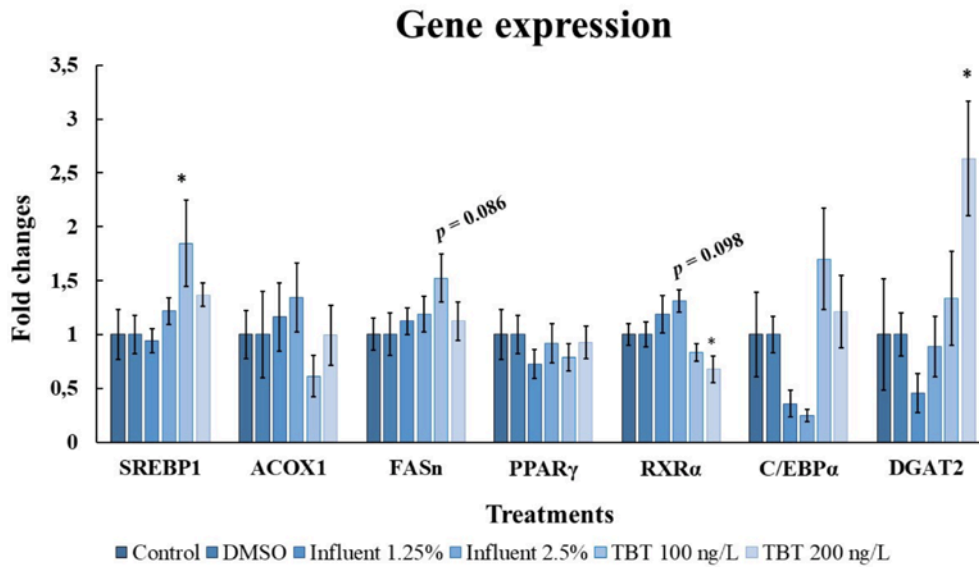
340 A statistically significant increase ( $p < 0.05$ ) in fluorescence was detected in larvae  
341 chronically exposed to the environmentally-relevant concentrations of 100 and 200 ng/L Sn  
342 TBT and 2.5% WWTP influent, with WAT deposits concentrating in the perivisceral area.  
343 Whereas the subcutaneous fat accumulation is considered an adaptive process, exceeding  
344 the storage capacity of this adipose depot, diverts the excess of fatty acids towards the  
345 accumulation in the visceral cavity, muscle and liver, primary locations for correlations  
346 with metabolic disorders and increased mortality (Chamorro-Garcia and Blumberg, 2014;  
347 Grün and Blumberg, 2009; Lyssimachou *et al.*, 2015).

348 Preliminary assays performed by our group with regular diet (Gemma Micro, 59%  
349 protein, 19% oil) did not lead to an increase in fat accumulation in TBT exposed larvae  
350 (data not shown). Hence, the assays were performed with a SD supplied with additional  
351 lipids (25% of lipid content). Tingaud-Sequeira and colleagues (2011), reared zebrafish  
352 larvae on a standard diet and separated them into two groups which were fed for a day with  
353 different diets, SD or hard-boiled egg yolk as an HFD, followed by two days of starvation.  
354 During starvation, the initial adiposity was recorded and larvae were posteriorly exposed for  
355 24h to 50 nM TBT and 1 nM rosiglitazone, with a final adiposity recording. The results  
356 indicated that HFD led to a more dramatic increase in lipid adiposity when the fishes were  
357 exposed, being more evident in the treatment with rosiglitazone in which, despite the fasting  
358 state, an increase in adiposity was obtained in the HFD group, oppositely to the smaller  
359 decrease recorded for the SD group when compared to the control. The present study  
360 corroborates previous findings of short-term exposures to higher TBT concentrations  
361 (Tingaud-Sequeira *et al.*, 2011) and to life-cycle zebrafish exposure to 10 and 50 ng/TBT  
362 (Lyssimachou *et al.*, 2015). Similarly, zebrafish larvae exposed for 15 days to  
363 tetrabromobisphenol A (TBBPA), tetrachlorobisphenol A, TBBPA-sulfate or TBT, and fed

364 with egg yolk, exhibited significant increases in lipid accumulation (Riu *et al.*, 2014). The  
365 authors also pointed out that when the larvae were fed with regular diets, instead of HFD,  
366 none of the treatments resulted in the staining of larvae, highlighting the impact of the  
367 synergy of both calories and chemical exposure in lipid accumulation.

368 As fat build-up results from the balance between lipogenesis and lipolysis (Kersten,  
369 2001), this study assessed the impact of TBT and the WWTP influent on both lipogenesis  
370 and adipogenesis focusing in particular in PPAR $\gamma$ :RXR $\alpha$  associated pathways  
371 (i.e., PPAR $\gamma$ :RXR $\alpha$ , SREBP1, C/EBP $\alpha$ , FASN, DGAT2) and also fatty acid oxidation  
372 (ACOX1). Bodies of zebrafish larvae from the *in vivo* assay were analyzed by qPCR to  
373 determine whether the lipid accumulation verified *in vivo* was accompanied by changes in  
374 levels of mRNA of key transcription factors and enzymes ruling lipid homeostasis.

375 Interestingly, the PCR results (**Figure 3**) only reveal statistically significant differences  
376 in the expression of the transcription factor SREBP1 at 100 ng/L Sn TBT and RXR $\alpha$   
377 alongside DGAT2 at 200 ng/L Sn TBT, environmental concentrations that triggered  
378 significant lipid accumulations *in vivo*. Both the increase of SREBP1 levels at the lowest  
379 concentration and decrease of RXR $\alpha$  expression levels at the highest concentration, suggest  
380 a mechanism of negative feedback, whereas the overexpression of DGAT2, the enzyme that  
381 catalyzes the final reaction in triglyceride's synthesis (Lyssimachou *et al.*, 2015), suggests  
382 that lipid production has not ceased at the highest concentration of TBT. While the lack of  
383 altered significant gene expression for 1.25% influent matches the observed lack of lipid  
384 accumulation, the similar observation for the 2.5% concentration, which contrastingly  
385 induced significant accumulation, could also be due to a negative feedback mechanism.  
386 This could explain the 3-fold decrease in gene expression of C/EBP $\alpha$  in larvae exposed to  
387 both WWTP influent treatments.



389

390 **Figure 3. *In vivo* induction of lipogenic and adipogenic genes in zebrafish, following**  
 391 **exposure to TBT and WWTP influents.** Values normalized to  $\beta$ -actin and relative to an  
 392 internal calibrator are expressed as the average fold changes  $\pm$  SEM of the solvent control  
 393 and experimental control groups for TBT and the WWTP influents, respectively. \* $p < 0.05$   
 394 (one-way ANOVA, followed by Fisher LSD's test).

395 Similarly, Watt and Schlezinger (2015) reported lipid accumulations in bone marrow  
 396 MSCs of male 9-week-old C57BL/6J mice following exposure to PPAR $\gamma$ -agonists  
 397 rosiglitazone, TBT and triphenyltin, with no statistical significant increases in PPAR $\gamma$   
 398 mRNA, although downstream target genes were up-regulated (Watt & Schlezinger, 2015).  
 399 Whereas PPAR $\gamma$  plays an important role in lipogenesis and adipogenesis in the adipose  
 400 tissue, the levels of expression in other tissues are low, for example in the liver where the  
 401 main mediator of the expression of lipogenic genes is SREBP-1 (Kersten, 2001). Thus, it is  
 402 not surprising that several studies report organ-specific and sex-specific effects of exposure  
 403 to TBT and other lipid homeostasis regulators in a variety of model animals (Bian *et al.*,

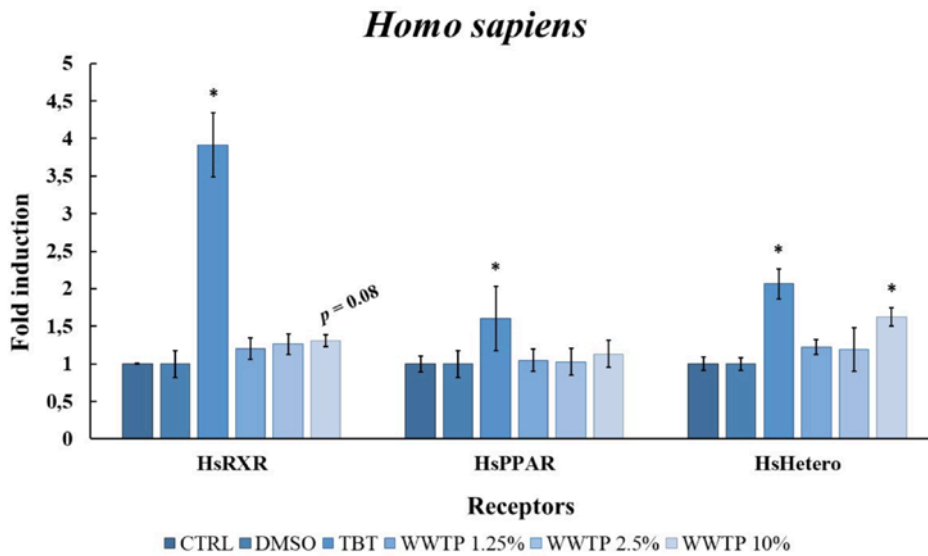
404 2017; Chamorro-García *et al.*, 2013; Guan *et al.*, 2016; Lyssimachou *et al.*, 2015; Zhang *et*  
405 *al.*, 2012).

406 Nevertheless, the transcription factor SREBP1, which was overexpressed at 100 ng/L  
407 Sn TBT, is an early regulator of adipogenesis and stimulates PPAR $\gamma$  expression for the final  
408 adipocyte maturation where they will modulate the expression of adipogenic and lipogenic  
409 enzymes, such as ACC $\alpha$  and FASn (Birsoy *et al.*, 2013; Capitão *et al.*, 2017; Kersten, 2001;  
410 Lyssimachou *et al.*, 201; Moseti *et al.*, 2016; Santos *et al.*, 2012).

### 411 3.2. Transactivation assays

412 To further address if the WWTP influent and TBT could transactivate or repress the  
413 PPAR $\gamma$ /RXR $\alpha$  signaling pathways, we have performed transactivation assays using human  
414 (Hs) and zebrafish (Dre) PPAR $\gamma$  and RXR $\alpha$  receptors, as well as with the RXR $\alpha$ :PPAR $\gamma$   
415 heterodimer. The results indicate that both influent and TBT are able to interact with the  
416 receptors *in vitro*, which might possibly be one of the mechanisms underlying the observed  
417 lipid accumulation and disruption of lipid homeostasis *in vivo*. The organotin TBT was the  
418 first obesogen to be associated with RXR and PPAR $\gamma$  signaling (Janesick and Blumberg,  
419 2011; Santos *et al.*, 2012). Indeed, our positive control TBT transactivated HsRXR $\alpha$ ,  
420 PPAR $\gamma$  and heterodimer at 250 nM (**Figure 4**). Interestingly, the results for the zebrafish  
421 receptors (**Figure 5**) show a different response when compared to HsPPAR $\gamma$ . While  
422 DreRXR $\alpha$  activity was significantly induced and PPAR $\gamma$  not affected by TBT, the  
423 heterodimer was massively repressed at the tested concentration.

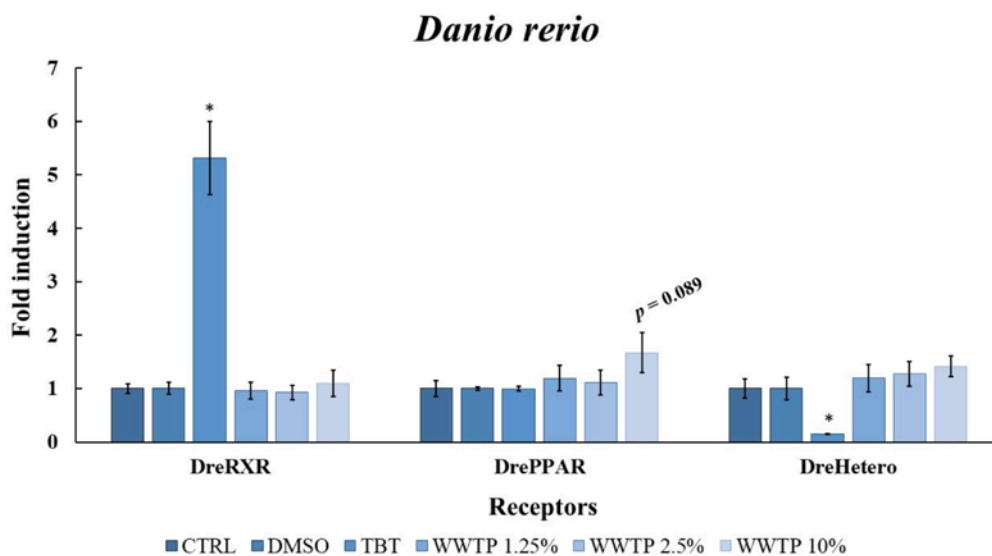
424



425

426 **Figure 4.** *In vitro* transactivation of *Homo sapiens* receptors by 250 nM TBT and WWTP  
427 **influent.** The activity of firefly luciferase (*Photinus pyralis*) was normalized to the activity  
428 of *Renilla* luciferase (*Renilla reniformis*) and then expressed as average fold changes  $\pm$  SEM  
429 of the solvent control group. \* $p < 0.05$  (one-way ANOVA, followed by Fisher's LSD test).

430



431

432 **Figure 5. *In vitro* transactivation of *Danio rerio* receptors by 250 nM TBT and WWTP**  
433 **influent.** The activity of firefly luciferase (*Photinus pyralis*) was normalized to the activity  
434 of *Renilla* luciferase (*Renilla reniformis*) and then expressed as average fold changes  $\pm$  SEM  
435 of the solvent control group. \* $p < 0.05$  (one-way ANOVA, followed by Fisher's LSD test).

436 Analyzing the amino acid sequences of human and zebrafish receptors, it was found a  
437 high percentage of similarities (99%) in both RXR $\alpha$  DNA-binding domain (DBD) and  
438 LBD, oppositely to the 94% similarities at the PPAR $\gamma$  DBD and 74% at the LBD (Ouadah-  
439 Boussouf & Babin, 2016; Zhao *et al.*, 2015), suggesting different ligand-binding affinities  
440 for PPAR $\gamma$ . Furthermore, the cysteine in position 285 of HsPPAR $\gamma$  LBD, which is mutated  
441 into a tyrosine in the zebrafish (Capitão *et al.*, 2017), has been shown as essential for the  
442 activation of this receptor by TBT (Harada *et al.*, 2015). This mutation could underlie the  
443 disparity between the transactivation results, as differences in nuclear receptors' structures  
444 may lead to distinct chemical binding and activation outcomes (Capitão *et al.*, 2017). The  
445 underlying mechanism of this finding has been recently discussed by Capitão *et al.*, (2018).

446 Indeed, Riu and collaborators have also noted that known HsPPAR $\gamma$  agonists  
447 thiazolidinediones (rosiglitazone, pioglitazone, ciglitazone and troglitazone), TBT and a  
448 prostaglandin could not be used as positive controls in assays involving DrePPAR $\gamma$ , as they  
449 failed to activate the receptor *in vitro* (Riu *et al.*, 2014).

450 The lack of DrePPAR $\gamma$  transactivation in comparison to RXR $\alpha$  suggest that the TBT's  
451 obesogenic effects reported here might be mediated by RXR $\alpha$  instead. In fact, this chemical  
452 was also reported to interact with other permissive heterodimers (LXR:RXR $\alpha$  heterodimer)  
453 (Capitão *et al.*, 2017; Le Maire *et al.*, 2009) and it has been suggested that the covalent  
454 binding to HsRXR $\alpha$ 's Cys432 would allow a more efficient stabilization of the active  
455 receptor conformation, than its non-covalent ionic bond to HsPPAR $\gamma$ 's Cys285 (Harada *et*  
456 *al.*, 2015; Le Maire *et al.*, 2009). Ouadah-Boussouf and Babin (2016) demonstrated that the

457 obesogenic effect of TBT on DreRXR:PPAR $\gamma$  was not inhibited by the HsPPAR $\gamma$   
458 antagonist T0070907, but was fully abolished by the HsRXR antagonist UVI3003 and by a  
459 combination of HsRXR:RXR and HsRXR:PPAR $\gamma$  antagonists. The findings of Ouadah-  
460 Boussouf and Babin (2016) support that RXR plays a central role in TBT-modulated  
461 obesogenic outcomes and that *in vivo* obesogenic effects might occur through RXR-  
462 dependent pathways which do not necessarily involve PPAR isoforms (Ouadah-Boussouf &  
463 Babin, 2016).

464 TBT may modulate other NRs involved in lipid homeostasis such as LXR:RXR  
465 heterodimer (Capitão *et al.*, 2017; Le Maire *et al.*, 2009). Interestingly, LXR is tightly  
466 related to cholesterol homeostasis and regulates the expression of SREBP-1 (Capitão *et al.*,  
467 2017), one of the upregulated target genes after exposure to TBT at 100 ng/L Sn.  
468 Regardless, unveiling the crystallographic structure of TBT binding to the human RXR and  
469 PPAR $\gamma$  has allowed a better understanding of the interaction with these receptors. Similar  
470 studies should be performed with other chemicals and nuclear receptors to help elucidate  
471 the different species-responses to a particular lipid homeostasis regulator.

472 Regarding the environmental samples, only the highest tested influent concentration (10%)  
473 was able to significantly transactivate the heterodimer HsPPAR $\gamma$ /RXR $\alpha$ , thus indicating the  
474 presence in the influent of HsPPAR $\gamma$ /RXR $\alpha$  agonists (**Figure 4**). It is important to have in  
475 mind that the tested concentrations of 1.25% and 2.5% were used when zebrafish larvae  
476 were chronically exposed from the 4<sup>th</sup> to the 18<sup>th</sup> dpf *in vivo*. Thus, the results are not easily  
477 comparable, as transactivation assays comprise a short 24-hour window of exposure, which  
478 could explain the lack of transactivation at these lower concentrations. In DrePPAR $\gamma$  a 1.5-  
479 fold induction was observed for the 10% influent concentrations, although differences did  
480 reach significance in comparison with control ( $p = 0.089$ ).

481 A simultaneous exposure to a “cocktail” of chemicals can potentially lead to additive or  
482 even synergistic effects (e.g. by acting on both RXR and PPAR $\gamma$  simultaneously) (Biemann

483 *et al.*, 2014; Riu *et al.*, 2011) but also to antagonistic effects. Since several compounds have  
484 also been shown to repress the transactivation of nuclear receptors involved in lipid  
485 homeostasis, the possibility of antagonistic actions of different chemicals on the nuclear  
486 receptors cannot be disregarded (Biemann *et al.*, 2014). Indeed, the chemical  
487 characterization of the influent used in this study (**Appendix A**, Table S1) shows the  
488 presence of a variety of chemicals that have been reported to impact lipid homeostasis  
489 triggering lipid storage, i.e., (diclofenac (Puhl *et al.*, 2015), ibuprofen (Puhl *et al.*, 2015),  
490 dibutyl phthalate (Mjaeed *et al.*, 2017), methyl paraben (Hu *et al.*, 2016), acesulfame (Bian  
491 *et al.*, 2017), saccharin (Suez *et al.*, 2015)) or lipid mobilization, i.e., (metformin (Park *et*  
492 *al.*, 2009), piperine (Shah *et al.*, 2011), irbesartan (Parhofer *et al.*, 2007), valsartan (Cole *et*  
493 *al.*, 2010), chenodioli (Chen *et al.*, 2017), hippuric acid (Zhao *et al.*, 2016), fenofibric acid  
494 (Alagona, 2010)). Some of the compounds present in the influent have been reported to  
495 interact with the PPAR/RXR receptors, either through induction and/or agonism [PPAR $\gamma$ :  
496 acesulfame (Simon *et al.*, 2013), saccharin (Simon *et al.*, 2013), irbesartan (Afzal *et al.*,  
497 2016), valsartan (Hasan *et al.*, 2014; Storka *et al.*, 2008), diclofenac (Ayoub *et al.*, 2009;  
498 Puhl *et al.*, 2015), ibuprofen (Puhl *et al.*, 2015), dibutyl phthalate (Lapinskas *et al.*, 2005;  
499 Pereira-Fernandes *et al.*, 2013), metformin (Elia *et al.*, 2011); methyl paraben (Pereira-  
500 Fernandes *et al.*, 2013); PPAR $\alpha$ : metformin (Maida *et al.*, 2011); dibutyl phthalate  
501 (Lapinskas *et al.*, 2005), irbesartan (Rong *et al.*, 2010); fenofibric acid (Qiu *et al.*, 2017);  
502 Mouse PPAR $\alpha$ : triclosan (Wu *et al.*, 2014);] or suppression and/or antagonism [PPAR $\gamma$ :  
503 piperine (Park *et al.*, 2012); PPAR $\alpha$ : chenodioli (Chen *et al.*, 2017); human PPAR $\alpha$ :  
504 triclosan (Wu *et al.*, 2014)].

505 The preliminary mechanistic approach performed here to address the involvement of the  
506 PPAR $\gamma$ /RXR $\alpha$  in the lipid accumulation observed *in vivo* in the 2.5% influent exposed  
507 larvae is not fully conclusive. Even though the chemical analysis of our environmental

508 samples confirms the presence of known PPAR $\gamma$  agonists and antagonists, it seems likely  
509 that other mechanisms might have also directed the *in vivo* effects observed.

510 So far, very few studies reported the impact of chemical mixtures and environmental  
511 samples on obesity and metabolic endpoints (Adeogun *et al.*, 2016; Biemann *et al.*, 2014;  
512 Lyche *et al.*, 2013, 2011; Maisano *et al.*, 2016), which is concerning, as only the exposure  
513 to mixtures depict real-case scenarios and the results are not always predictable by the  
514 effects of the individual compounds alone (Biemann *et al.*, 2014; Rodrigues *et al.*, 2006;  
515 Santos *et al.*, 2006, 2008; Sarria *et al.*, 2011). In addition to organotins, other groups of  
516 compounds have been investigated for their variety of MoA on obesity outcomes and lipid  
517 homeostasis disruption: primary phthalates, such as (2-ethylhexyl) phthalate (DEHP),  
518 activate PPAR $\alpha$ , favoring a lipolysis state, whereas their metabolites show preference for  
519 PPAR $\gamma$  (Grün & Blumberg, 2009); Halogenated Bisphenol A derivatives have been shown  
520 to disrupt the thyroid hormone receptor, estrogen receptors and the PPAR $\gamma$  signaling (Bašić  
521 *et al.*, 2012; Riu *et al.*, 2011). As lipogenesis and adipogenesis involve a complex network  
522 of transcription factors and enzymes, the disruption of the energy homeostasis can occur at  
523 many levels (Bašić *et al.*, 2012). Weighting these different factors together, through the  
524 study of complex samples of chemicals, is important to obtain a more realistic assessment  
525 of the impact of these mixtures on animal and human health. Interestingly, epidemiological  
526 and toxicological studies show a moderate to strong probability of human obesity being  
527 associated with exposure to DDE, Di-2-ethylhexylphthalate and BPA (Trasande *et al.*,  
528 2015).

#### 529 **4. CONCLUSION**

530 The present study demonstrates, for the first time, obesogenic responses in zebrafish  
531 larvae following exposure to complex environmental samples reported to contain an array  
532 of chemicals known to modulate lipid homeostasis. Yet, the mechanistic studies performed  
533 here are not fully conclusive. Hence, future studies should expand the screening to

534 additional nuclear receptors known to be engaged in vertebrate's lipid homeostasis and the  
535 study of pathway's other than the ones regulated by PPAR $\gamma$ /RXR $\alpha$ .

#### 536 **DECLARATION OF INTEREST**

537 Conflicts of interest: none.

538

#### 539 **ACKNOWLEDGMENTS**

540 This work was supported by the Norte2020 and FEDER (Coral—Sustainable Ocean  
541 Exploitation—Norte-01-0145-FEDER-000036), the Spanish Agencia Estatal de  
542 Investigación (CTM2017-84763-C3-2-R), the Galician Council of Culture, Education and  
543 Universities (ED431C2017/36) and FEDER/ERDF.

544

#### 545 **REFERENCES**

546 Adeogun, A.O., Ibor, O.R., Regoli, F., Arukwe, A., 2016. Peroxisome proliferator-  
547 activated receptors and biotransformation responses in relation to condition factor  
548 and contaminant burden in tilapia species from Ogun River, Nigeria. *Comp.*  
549 *Biochem. Physiol. Part - C Toxicol. Pharmacol.* 183–184, 7–19.

550 <https://doi.org/10.1016/j.cbpc.2015.12.006>

551 Afzal, S., Sattar, M.A., Johns, E.J., Abdulla, M.H., Akhtar, S., Hashmi, F., Abdullah,  
552 N.A., 2016. Interaction between irbesartan, peroxisome proliferator-activated  
553 receptor (PPAR- $\gamma$ ), and adiponectin in the regulation of blood pressure and renal  
554 function in spontaneously hypertensive rats. *J. Physiol. Biochem.* 72, 593–604.

555 <https://doi.org/10.1007/s13105-016-0497-1>

556 Alagona, P., 2010. Fenofibric acid: A new fibrate approved for use in combination with  
557 statin for the treatment of mixed dyslipidemia. *Vasc. Health Risk Manag.* 6, 351–

558 362. <https://doi.org/10.2147/VHRM.S6714>

559 André, A., Ruivo, R., Capitão, A., Froufe, E., Páscoa, I., Castro, L.F.C., Santos, M.M.,

560 2017. Cloning and functional characterization of a retinoid X receptor orthologue  
561 in *Platynereis dumerilii*: An evolutionary and toxicological perspective.  
562 Chemosphere 182, 753–761. <https://doi.org/10.1016/j.chemosphere.2017.05.064>

563 Ayoub, S.S., Botting, R.M., Joshi, A.N., Seed, M.P., Colville-Nash, P.R., 2009.  
564 Activation of macrophage peroxisome proliferator-activated receptor- $\gamma$  by  
565 diclofenac results in the induction of cyclooxygenase-2 protein and the synthesis of  
566 anti-inflammatory cytokines. Mol. Cell. Biochem. 327, 101–110.  
567 <https://doi.org/10.1007/s11010-009-0048-y>

568 Bašić, M., Butorac, A., Jurčević, I. L., Bačun-Družina, V., 2012. Obesity: genome and  
569 environment interactions. Arh. Hig. Rada Toksikol. 63, 395–405.  
570 <https://doi.org/10.2478/10004-1254-63-2012-2244>

571 Bian, X., Chi, L., Gao, B., Tu, P., Ru, H., Lu, K., 2017. The artificial sweetener  
572 acesulfame potassium affects the gut microbiome and body weight gain in CD-1  
573 mice. PLoS One 12, 1–16. <https://doi.org/10.1371/journal.pone.0178426>

574 Biemann, R., Fischer, B., Navarrete Santos, A., 2014. Adipogenic effects of a  
575 combination of the endocrine-disrupting compounds bisphenol a,  
576 diethylhexylphthalate, and tributyltin. Obes. Facts 7, 48–56.  
577 <https://doi.org/10.1159/000358913>

578 Birsoy, K., Festuccia, W.T., Laplante, M., 2013. A comparative perspective on lipid  
579 storage in animals. J. Cell Sci. 126, 1541–1552. <https://doi.org/10.1242/jcs.104992>

580 Capitão, A., Lyssimachou, A., Castro, L.F.C., Santos, M.M., 2017. Obesogens in the  
581 aquatic environment: an evolutionary and toxicological perspective. Environ. Int.  
582 106, 153–169. <https://doi.org/10.1016/j.envint.2017.06.003>

583 Capitão, A.M.F., Lopes-Marques, M.S., Ishii, Y., Ruivo, R., Fonseca, E.S.S., Páscoa, I.,  
584 Jorge, R.P., Barbosa, M.A.G., Hiromori, Y., Miyagi, T., Nakanishi, T., Santos,

585 M.M., Castro, L.F.C., 2018. Evolutionary Exploitation of Vertebrate Peroxisome  
586 Proliferator-Activated Receptor  $\gamma$  by Organotins. Environ. Sci. Technol. 52,  
587 13951–13959. <https://doi.org/10.1021/acs.est.8b04399>

588 Chamorro-García, R., Blumberg, B., 2014. Transgenerational effects of obesogens and  
589 the obesity epidemic. Curr. Opin. Pharmacol. 19, 153–158.  
590 <https://doi.org/10.1016/j.coph.2014.10.010>

591 Chamorro-García, R., Diaz-Castillo, C., Shoucri, B.M., Käch, H., Leavitt, R., Shioda,  
592 T., Blumberg, B., 2017. Ancestral perinatal obesogen exposure results in a  
593 transgenerational thrifty phenotype in mice. Nat. Commun. 8.  
594 <https://doi.org/10.1038/s41467-017-01944-z>

595 Chamorro-García, R., Sahu, M., Abbey, R.J., Laude, J., Pham, N., Blumberg, B., 2013.  
596 Transgenerational inheritance of increased fat depot size, stem cell reprogramming,  
597 and hepatic steatosis elicited by prenatal exposure to the obesogen tributyltin in  
598 mice. Environ. Health Perspect. 121, 359–366.  
599 <https://doi.org/10.1289/ehp.1205701>

600 Chen, X., Yan, L., Guo, Z., Chen, Y., Li, M., Huang, C., Chen, Z., Meng, X., 2017.  
601 Chenodeoxycholic acid attenuates high-fat diet-induced obesity and hyperglycemia  
602 via the G protein-coupled bile acid receptor 1 and proliferator-activated receptor  $\gamma$   
603 pathway. Exp. Ther. Med. 14, 5305–5312. <https://doi.org/10.3892/etm.2017.5232>

604 Coimbra, A.M., Peixoto, M.J., Coelho, I., Lacerda, R., Carvalho, A.P., Gesto, M.,  
605 Lyssimachou, A., Lima, D., Soares, J., André, A., Capitão, A., Castro, L.F.C.,  
606 Santos, M.M., 2015. Chronic effects of clofibric acid in zebrafish (*Danio rerio*): A  
607 multigenerational study. Aquat. Toxicol. 160, 76–86.  
608 <https://doi.org/10.1016/j.aquatox.2015.01.013>

609 Cole, B.K., Keller, S.R., Wu, R., Carter, J.D., Nadler, J.L., Nunemaker, C.S., 2010.

610 Valsartan protects pancreatic islets and adipose tissue from the inflammatory and  
611 metabolic consequences of a high-fat diet in mice. *Hypertension* 55, 715–721.  
612 <https://doi.org/10.1161/HYPERTENSIONAHA.109.148049>

613 Dimastrogiovanni, G., Córdoba, M., Navarro, I., Jáuregui, O., Porte, C., 2015.  
614 Alteration of cellular lipids and lipid metabolism markers in RTL-W1 cells  
615 exposed to model endocrine disrupters. *Aquat. Toxicol.* 165, 277–285.  
616 <http://dx.doi.org/10.1016/j.aquatox.2015.06.005>

617 Elia, E.M., Pustovrh, C., Amalfi, S., Devoto, L., Motta, A.B., 2011. Link between  
618 metformin and the peroxisome proliferator-activated receptor  $\gamma$  pathway in the  
619 uterine tissue of hyperandrogenized prepubertal mice. *Fertil. Steril.* 95, 2534–  
620 2537.e1. <https://doi.org/10.1016/j.fertnstert.2011.02.004>

621 González-Mariño, I., Zuccato, E., Santos, M.M., Castiglioni, S., 2017. Monitoring  
622 MDMA metabolites in urban wastewater as novel biomarkers of consumption.  
623 *Water Res.* 115, 1–8. <https://doi.org/10.1016/j.watres.2017.01.063>

624 Gracia-Lor, E., Rousis, N.I., Zuccato, E., Bade, R., Baz-Lomba, J.A., Castrignanò, E.,  
625 Causanilles, A., Hernández, F., Kasprzyk-Hordern, B., Kinyua, J., McCall, A.K.,  
626 van Nuijs, A.L.N., Plósz, B.G., Ramin, P., Ryu, Y., Santos, M.M., Thomas, K., de  
627 Voogt, P., Yang, Z., Castiglioni, S., 2017. Estimation of caffeine intake from  
628 analysis of caffeine metabolites in wastewater. *Sci. Total Environ.* 609, 1582–  
629 1588. <https://doi.org/10.1016/j.scitotenv.2017.07.258>

630 Grün, F., Blumberg, B., 2009. Minireview: The Case for Obesogens. *Mol. Endocrinol.*  
631 23, 1127–1134. <https://doi.org/10.1210/me.2008-0485>

632 Grün, F., Blumberg, B., 2007. Perturbed nuclear receptor signaling by environmental  
633 obesogens as emerging factors in the obesity crisis. *Rev. Endocr. Metab. Disord.* 8,  
634 161–171. <https://doi.org/10.1007/s11154-007-9049-x>

635 Guan, Y., Gao, J., Zhang, Y., Chen, S., Yuan, C., Wang, Z., 2016. Effects of bisphenol  
636 A on lipid metabolism in rare minnow *Gobiocypris rarus*. *Comp. Biochem.*  
637 *Physiol. Part - C Toxicol. Pharmacol.* 179, 144–149.  
638 <https://doi.org/10.1016/j.cbpc.2015.10.006>

639 Harada, S., Hiromori, Y., Nakamura, S., Kawahara, K., Fukakusa, S., Maruno, T.,  
640 Noda, M., Uchiyama, S., Fukui, K., Nishikawa, J., Nagase, H., Kobayashi, Y.,  
641 Yoshida, T., Ohkubo, T., Nakanishi, T., 2015. Structural basis for PPAR $\gamma$   
642 transactivation by endocrine-disrupting organotin compounds. *Sci. Rep.* 5, 8520.  
643 <https://doi.org/10.1038/srep08520>

644 Hasan, A.U., Ohmori, K., Hashimoto, T., Kamitori, K., Yamaguchi, F., Ishihara, Y.,  
645 Ishihara, N., Noma, T., Tokuda, M., Kohno, M., 2014. Valsartan ameliorates the  
646 constitutive adipokine expression pattern in mature adipocytes: A role for inverse  
647 agonism of the angiotensin II type 1 receptor in obesity. *Hypertens. Res.* 37, 621–  
648 628. <https://doi.org/10.1038/hr.2014.51>

649 Hill, A.J., Teraoka, H., Heideman, W., Peterson, R.E., 2005. Zebrafish as a model  
650 vertebrate for investigating chemical toxicity. *Toxicol. Sci.* 86, 6–19.  
651 <https://doi.org/10.1093/toxsci/kfi110>

652 Hölttä-Vuori, M., Salo, V.T.V., Nyberg, L., Brackmann, C., Enejder, A., Panula, P.,  
653 Ikonen, E., 2010. Zebrafish: gaining popularity in lipid research. *Biochem. J.* 429,  
654 235–242. <https://doi.org/10.1042/BJ20100293>

655 Hu, P., Kennedy, R.C., Chen, X., Zhang, J., Shen, C.L., Chen, J., Zhao, L., 2016.  
656 Differential effects on adiposity and serum marker of bone formation by post-  
657 weaning exposure to methylparaben and butylparaben. *Environ. Sci. Pollut. Res.*  
658 23, 21957–21968. <https://doi.org/10.1007/s11356-016-7452-0>

659 Janer, G., Navarro, J.C., Porte, C., 2007. Exposure to TBT increases accumulation of

660 lipids and alters fatty acid homeostasis in the ramshorn snail *Marisa cornuarietis*.  
661 *Comp. Biochem. Physiol., Part C: Toxicol. Pharmacol.* 146, 368–374.  
662 <https://doi.org/10.1016/j.cbpc.2007.04.009>

663 Janesick, A., Blumberg, B., 2011. Minireview: PPAR $\gamma$  as the target of obesogens. *J.*  
664 *Steroid Biochem. Mol. Biol.* 127, 4–8. <https://doi.org/10.1016/j.jsbmb.2011.01.005>

665 Jordão, R., Casas, J., Fabrias, G., Campos, B., Piña, B., Lemos, M.F.L., Soares,  
666 A.M.V.M., Tauler, R., Barata, C., 2015. Obesogens beyond vertebrates: lipid  
667 perturbation by tributyltin in the crustacean *Daphnia magna*. *Environ. Health*  
668 *Perspect.* 123, 813–819. <http://dx.doi.org/10.1289/ehp.1409163>.

669 Jordão, R.; Campos, B.; Pina, B.; Tauler, R.; Soares, A. M.; Barata, C. Mechanisms of  
670 Action of Compounds That Enhance Storage Lipid Accumulation in *Daphnia*  
671 *magna*. *Environ. Sci. Technol.* 2016, 50 (24), 13565–13573.  
672 <https://doi.org/10.1021/acs.est.6b04768>

673 Kersten, S., 2001. Mechanisms of nutritional and hormonal regulation of lipogenesis.  
674 *EMBO Rep.* 2, 282–286. <https://doi.org/10.1093/embo-reports/kve071>

675 Klimentidis, Y.C., Beasley, T. M., Lin, H.Y., Murati, G., Glass, G.E., Guyton, M.,  
676 Newton, W., Jorgensen, M., Heymsfield, S.B., Kemnitz, J., Fairbanks, L., Allison,  
677 D.B., 2011. Canaries in the coal mine: A cross-species analysis of the plurality of  
678 obesity epidemics. *Proc. R. Soc. B Biol. Sci.* 278, 1626–1632.  
679 <https://doi.org/10.1098/rspb.2010.1890>

680 Landgraf, K., Schuster, S., Meusel, A., Garten, A., Riemer, T., Schleinitz, D., Kiess,  
681 W., Körner, A., 2017. Short-term overfeeding of zebrafish with normal or high-fat  
682 diet as a model for the development of metabolically healthy versus unhealthy  
683 obesity. *BMC Physiol.* 17, 4. <https://doi.org/10.1186/s12899-017-0031-x>

684 Lapinskas, P.J., Brown, S., Leesnitzer, L.M., Blanchard, S., Swanson, C., Cattley, R.C.,

685 Corton, J.C., 2005. Role of PPAR $\alpha$  in mediating the effects of phthalates and  
686 metabolites in the liver. *Toxicology* 207, 149–163.  
687 <https://doi.org/10.1016/j.tox.2004.09.008>

688 le Maire, A., Grimaldi, M., Roecklin, D., Dagnino, S., Vivat-Hannah, V., Balaguer, P.,  
689 Bourguet, W., 2009. Activation of RXR-PPAR heterodimers by organotin  
690 environmental endocrine disruptors. *EMBO Rep.* 10, 367–373.  
691 <https://doi.org/10.1038/embor.2009.8>

692 Lempradl, A., Pospisilik, J.A., Penninger, J.M., 2015. Exploring the emerging  
693 complexity in transcriptional regulation of energy homeostasis. *Nat. Rev. Genet.*  
694 16, 665–681. <https://doi.org/10.1038/nrg3941>

695 Livak, K.J., Schmittgen, T.D., 2001. Analysis of Relative Gene Expression Data Using  
696 Real- Time Quantitative PCR and the  $2^{-\Delta\Delta C_T}$  Method. *METHODS* 25, 402–408.  
697 <https://doi.org/10.1006/meth.2001.1262>

698 Lyche, J.L., Grześ, I.M., Karlsson, C., Nourizadeh-Lillabadi, R., Berg, V.,  
699 Kristoffersen, A.B., Skåre, J.U., Alestrøm, P., Ropstad, E., 2013. Parental exposure  
700 to natural mixtures of POPs reduced embryo production and altered gene  
701 transcription in zebrafish embryos. *Aquat. Toxicol.* 126, 424–434.  
702 <https://doi.org/10.1016/j.aquatox.2012.08.019>

703 Lyche, J.L., Nourizadeh-Lillabadi, R., Karlsson, C., Stavik, B., Berg, V., Skåre, J.U.,  
704 Alestrøm, P., Ropstad, E., 2011. Natural mixtures of POPs affected body weight  
705 gain and induced transcription of genes involved in weight regulation and insulin  
706 signaling. *Aquat. Toxicol.* 102, 197–204.  
707 <https://doi.org/10.1016/j.aquatox.2011.01.017>

708 Lyssimachou, A., Santos, J.G., André, A., Soares, J., Lima, D., Guimarães, L., Almeida,  
709 C.M.R., Teixeira, C., Castro, L.F.C., Santos, M.M., 2015. The mammalian

710 “obesogen” tributyltin targets hepatic triglyceride accumulation and the  
711 transcriptional regulation of lipid metabolism in the liver and brain of zebrafish.  
712 PLoS One 10, 1–22. <https://doi.org/10.1371/journal.pone.0143911>

713 Maida, A., Lamont, B.J., Cao, X., Drucker, D.J., 2011. Metformin regulates the incretin  
714 receptor axis via a pathway dependent on peroxisome proliferator-activated  
715 receptor- $\alpha$  in mice. Diabetologia 54, 339–349. [https://doi.org/10.1007/s00125-010-](https://doi.org/10.1007/s00125-010-1937-z)  
716 [1937-z](https://doi.org/10.1007/s00125-010-1937-z)

717 Maisano, M., Cappello, T., Oliva, S., Natalotto, A., Giannetto, A., Parrino, V.,  
718 Battaglia, P., Romeo, T., Salvo, A., Spanò, N., Mauceri, A., 2016. PCB and OCP  
719 accumulation and evidence of hepatic alteration in the Atlantic bluefin tuna, *T.*  
720 *thynnus*, from the Mediterranean Sea. Mar. Environ. Res. 121, 40–48.  
721 <https://doi.org/10.1016/j.marenvres.2016.03.003>

722 Minchin, J.E.N., Rawls, J.F., 2011. *In vivo* Analysis of White Adipose Tissue in  
723 Zebrafish, in: Detrich III, W.H., Westerfield, M., Zon, L.I., (Eds.), The Zebrafish:  
724 Disease Models and Chemical Screens. Methods Cell Biol. 105, 63–86.  
725 <https://doi.org/10.1016/B978-0-12-381320-6.00003-5>

726 Mjaeed, K.A., ur Rehman, H., Yousaf, M.S., Zaneb, H., Rabbani, I., Tahir, S.K.,  
727 Rashid, M.A., 2017. Sub-chronic exposure to low concentration of dibutyl  
728 phthalate affects anthropometric parameters and markers of obesity in rats.  
729 Environ. Sci. Pollut. Res. 24, 25462–25467. [https://doi.org/10.1007/s11356-017-](https://doi.org/10.1007/s11356-017-9952-y)  
730 [9952-y](https://doi.org/10.1007/s11356-017-9952-y)

731 Moseti, D., Regassa, A., Kim, W.K., 2016. Molecular regulation of adipogenesis and  
732 potential anti-adipogenic bioactive molecules. Int. J. Mol. Sci. 17, 1–24.  
733 <https://doi.org/10.3390/ijms17010124>

734 Newbold, R.R., Padilla-Banks, E., Snyder, R.J., Phillips, T.M., Jefferson, W.N., 2007.

735        Developmental Exposure to Endocrine Disruptors and the Obesity Epidemic.  
736        Reprod. Toxicol. 23, 290–296. <https://doi.org/10.1016/j.reprotox.2006.12.010>

737    Ouadah-Boussouf, N., Babin, P.J., 2016. Pharmacological evaluation of the mechanisms  
738        involved in increased adiposity in zebrafish triggered by the environmental  
739        contaminant tributyltin. Toxicol. Appl. Pharmacol. 294, 32–42.  
740        <https://doi.org/10.1016/j.taap.2016.01.014>

741    Parhofer, K.G., Münzel, F., Krekler, M., 2007. Effect of the angiotensin receptor  
742        blocker irbesartan on metabolic parameters in clinical practice: The DO-IT  
743        prospective observational study. Cardiovasc. Diabetol. 6, 1–6.  
744        <https://doi.org/10.1186/1475-2840-6-36>

745    Park, U.H., Jeong, H.S., Jo, E.Y., Park, T., Yoon, S.K., Kim, E.J., Jeong, J.C., Um, S.J.,  
746        2012. Piperine, a component of black pepper, inhibits adipogenesis by  
747        antagonizing PPAR $\gamma$  activity in 3T3-L1 cells. J. Agric. Food Chem. 60, 3853–  
748        3860. <https://doi.org/10.1021/jf204514a>

749    Pereira-Fernandes, A., Demaegdt, H., Vandermeiren, K., Hectors, T.L.M., Jorens, P.G.,  
750        Blust, R., Vanparys, C., 2013. Evaluation of a Screening System for Obesogenic  
751        Compounds: Screening of Endocrine Disrupting Compounds and Evaluation of the  
752        PPAR Dependency of the Effect. PLoS One 8, 1–17.  
753        <https://doi.org/10.1371/journal.pone.0077481>

754    Puhl, A.C., Milton, F.A., Cvorov, A., Sieglaff, D.H., Campos, J.C.L., Bernardes, A.,  
755        Filgueira, C.S., Lindemann, J.L., Deng, T., Neves, F.A.R., Polikarpov, I., Webb,  
756        P., 2015. Mechanisms of peroxisome proliferator activated receptor  $\gamma$  regulation by  
757        non-steroidal anti-inflammatory drugs. Nucl. Recept. Signal. 13, 1–17.  
758        <https://doi.org/10.1621/nrs.13004>

759    Qiu, F., Matlock, G., Chen, Q., Zhou, K., Du, Y., Wang, X., Ma, J.X., 2017.

760 Therapeutic effects of PPAR $\alpha$  agonist on ocular neovascularization in models  
761 recapitulating neovascular age-related macular degeneration. *Investig. Ophthalmol.*  
762 *Vis. Sci.* 58, 5065–5075. <https://doi.org/10.1167/iovs.17-22091>

763 Riu, A., Grimaldi, M., le Maire, A., Bey, G., Phillips, K., Boulahtouf, A., Perdu, E.,  
764 Zalko, D., Bourguet, W., Balaguer, P., 2011. Peroxisome proliferator-activated  
765 receptor  $\gamma$  is a target for halogenated analogs of bisphenol A. *Environ. Health*  
766 *Perspect.* 119, 1227–1232. <https://doi.org/10.1289/ehp.1003328>

767 Riu, A., McCollum, C.W., Pinto, C.L., Grimaldi, M., Hillenweck, A., Perdu, E., Zalko,  
768 D., Bernard, L., Laudet, V., Balaguer, P., Bondesson, M., Gustafsson, J.A., 2014.  
769 Halogenated bisphenol-a analogs act as obesogens in zebrafish larvae (*Danio*  
770 *rerio*). *Toxicol. Sci.* 139, 48–58. <https://doi.org/10.1093/toxsci/kfu036>

771 Rodrigues, P., Reis-Henriques, M.A., Campos, J., Santos, M.M., 2006. Urogenital  
772 Papilla feminization in male *Pomatoschistus minutus* from two estuaries in  
773 northwestern Iberian Peninsula. *Mar. Environ. Res.* 62 (1): S258-S262.  
774 <https://doi.org/10.1016/j.marenvres.2006.04.032>

775 Rong, X., Li, Y., Ebihara, K., Zhao, M., Kusakabe, T., Tomita, T., Murray, M., Nakao,  
776 K., 2010. Irbesartan treatment up-regulates hepatic expression of PPAR and its  
777 target genes in obese Koletsky (fa<sup>k</sup>/fa<sup>k</sup>) rats: A link to amelioration of  
778 hypertriglyceridaemia. *Br. J. Pharmacol.* 160, 1796–1807.  
779 <https://doi.org/10.1111/j.1476-5381.2010.00835.x>

780 Santos, M.M., Micael, J., Carvalho, A.P., Morabito, R., Booy, P., Massanisso, P.,  
781 Lamoree, M., Reis-Henriques, M.A., 2006. Estrogens counteract the masculinizing  
782 effect of tributyltin in zebrafish. *Comp Biochem Physiol C* 142, 151-155.  
783 <https://doi.org/10.1016/j.cbpc.2005.11.014>

784 Santos, M.M., M.A. Reis-Henriques, R. Guillot, D. Lima, R. Franco-Duarte, I. Mendes,

785 S. Queirós, L. Filipe C. Castro, 2008. Anti-androgenic effects of sewage treatment  
786 plant effluents in the prosobranch gastropod *Nucella lapillus*. *Comp Biochem*  
787 *Physiol C* 148, 87-93. <https://doi.org/10.1016/j.cbpc.2008.03.012>

788 Santos, M.M., Reis-Henriques, M.A., Castro, L.F.C., 2012. Lipid homeostasis  
789 perturbation by organotins: effects on vertebrates and invertebrates, in: Pagliarani,  
790 A., Trombetti, F., Ventrella, V. (Eds.), *Biochemical and Biological Effects of*  
791 *Organotins*. Bentham Science Publishers, Sharjah, 83-96.  
792 <https://doi.org/10.2174/978160805265311201010083>

793 Santos, M.M., Ruivo, R., Capitão, A., Fonseca, E., Castro, L.F.C., 2018. Identifying the  
794 gaps: Resources and perspectives on the use of nuclear receptor based-assays to  
795 improve hazard assessment of emerging contaminants. *J. Hazard. Mater.* 358, 508–  
796 511. <https://doi.org/10.1016/j.jhazmat.2018.04.076>

797 Sárria, M.P., Santos, M.M., Reis-Henriques, M.A., Vieira, N.M., Monteiro, N.M., 2011.  
798 The unpredictable effects of mixtures of androgenic and estrogenic chemicals on  
799 fish early life. *Environ. Int.* 37(2):418-24.  
800 <https://doi.org/10.1016/j.envint.2010.11.004>

801 Simon, B.R., Parlee, S.D., Learman, B.S., Mori, H., Scheller, E.L., Cawthorn, W.P.,  
802 Ning, X., Gallagher, K., Tyrberg, B., Assadi-Porter, F.M., Evans, C.R.,  
803 MacDougald, O.A., 2013. Artificial sweeteners stimulate adipogenesis and  
804 suppress lipolysis independently of sweet taste receptors. *J. Biol. Chem.* 288,  
805 32475–32489. <https://doi.org/10.1074/jbc.M113.514034>

806 Schymanski, E.L., Jeon, J., Gulde, R., Fenner, K., Ruff, M., Singer, H.P., Hollender, J.,  
807 2014. Identifying Small Molecules via High Resolution Mass Spectrometry:  
808 Communicating Confidence *Environ. Sci. Technol.* 48, 2097–2098.  
809 <https://pubs.acs.org/doi/abs/10.1021/es5002105>

810 Spencer, S.J., Tilbrook, A., 2011. The glucocorticoid contribution to obesity. *Stress* 14,  
811 233–246. <https://doi.org/10.3109/10253890.2010.534831>

812 Storka, A., Vojtassakova, E., Mueller, M., Kapiotis, S., Haider, D.G., Jungbauer, A.,  
813 Wolzt, M., 2008. Angiotensin inhibition stimulates PPAR $\gamma$  and the release of  
814 visfatin. *Eur. J. Clin. Invest.* 38, 820–826. [https://doi.org/10.1111/j.1365-  
815 2362.2008.02025.x](https://doi.org/10.1111/j.1365-2362.2008.02025.x)

816 Suez, J., Korem, T., Zilberman-Schapira, G., Segal, E., Elinav, E., 2015. Non-caloric  
817 artificial sweeteners and the microbiome: Findings and challenges. *Gut Microbes*  
818 6, 149–155. <https://doi.org/10.1080/19490976.2015.1017700>

819 Tingaud-Sequeira, A., Ouadah, N., Babin, P.J., 2011. Zebrafish obesogenic test: a tool  
820 for screening molecules that target adiposity. *J. Lipid Res.* 52, 1765–1772.  
821 <https://doi.org/10.1194/jlr.D017012>

822 Trasande, L., Zoeller, R.T., Hass, U., Kortenkamp, A., Grandjean, P., Myers, J.P.,  
823 Digangi, J., Bellanger, M., Hauser, R., Legler, J., Skakkebaek, N.E., Heindel, J.J.,  
824 2015. Estimating burden and disease costs of exposure to endocrine-disrupting  
825 chemicals in the European Union. *J. Clin. Endocrinol. Metab.* 100, 1245–1255.  
826 <https://doi.org/10.1210/jc.2014-4324>

827 van Beekum, O., Fleskens, V., Kalkhoven, E., 2009. Posttranslational Modifications of  
828 PPAR- $\gamma$ : Fine-tuning the Metabolic Master Regulator. *Obesity* 17, 213–219.  
829 <https://doi.org/10.1038/oby.2008.473>

830 Veldman, M.B., Lin, S., 2008. Zebrafish as a developmental model organism for  
831 pediatric research. *Pediatr. Res.* 64, 470–476.  
832 <https://doi.org/10.1203/PDR.0b013e318186e609>

833 Wang, Y., Sul, H.S., 2013. Transcriptional regulation of lipogenesis and its contribution  
834 to hepatosteatosis. *Clin. Lipidol.* 8, 165–168. <https://doi.org/10.2217/clp.13.11>

835 Wang, Y., Viscarra, J., Kim, S.J., Sul, H.S., 2015. Transcriptional regulation of hepatic  
836 lipogenesis. *Nat. Rev. Mol. Cell Biol.* 16, 678–689.  
837 <https://doi.org/10.1038/nrm4074>

838 Watt, J., Schlezinger, J.J., 2015. Structurally-diverse, PPAR $\gamma$ -activating environmental  
839 toxicants induce adipogenesis and suppress osteogenesis in bone marrow  
840 mesenchymal stromal cells. *Toxicology* 331, 66–77.  
841 <https://doi.org/10.1016/j.tox.2015.03.006>

842 Wu, Y., Wu, Q., Beland, F.A., Ge, P., Manjanatha, M.G., Fang, J.L., 2014. Differential  
843 effects of triclosan on the activation of mouse and human peroxisome proliferator-  
844 activated receptor alpha. *Toxicol. Lett.* 231, 17–28.  
845 <https://doi.org/10.1016/j.toxlet.2014.09.001>

846 Yoon, M., 2009. The role of PPAR $\alpha$  in lipid metabolism and obesity: Focusing on the  
847 effects of estrogen on PPAR $\alpha$  actions. *Pharmacol. Res.* 60, 151–159.  
848 <https://doi.org/10.1016/j.phrs.2009.02.004>

849 Zhang, W., Zhang, Y., Zhang, H., Wang, J., Cui, R., Dai, J., 2012. Sex Differences in  
850 Transcriptional Expression of FABPs in Zebrafish Liver after Chronic  
851 Perfluorononanoic Acid Exposure. *Environ. Sci. Technol.* 46, 5175–5182.  
852 <https://doi.org/10.1021/es300147w>

853 Zhao, H., Shen, J., Djukovic, D., Daniel-MacDougall, C., Gu, H., Wu, X., Chow, W.H.,  
854 2016. Metabolomics-identified metabolites associated with body mass index and  
855 prospective weight gain among Mexican American women. *Obes. Sci. Pract.* 2,  
856 309–317. <https://doi.org/10.1002/osp4.63>

857 Zhao, Y., Zhang, K., Giesy, J.P., Hu, J., 2015. Families of Nuclear Receptors in  
858 Vertebrate Models: Characteristic and Comparative Toxicological Perspective. *Sci.*  
859 *Rep.* 5, 8554. <https://doi.org/10.1038/srep08554>

860

861

862

863

864

# **Linking chemical exposure to lipid homeostasis: a municipal waste water treatment plant influent is obesogenic for zebrafish larvae**

**Mélanie Audrey Barbosa <sup>a,b,c</sup>, Ricardo Capela, Jorge Rodolfo <sup>a,c</sup>, Elza Fonseca <sup>a</sup>, Rosa Montes <sup>d</sup>, Ana André <sup>a</sup>, Ana Capitão <sup>a</sup>, António Paulo Carvalho <sup>a,c</sup>, José Benito Quintana <sup>d</sup>, L. Filipe C. Castro <sup>a,b</sup>, Miguel Machado Santos <sup>a,b,\*</sup>**

## **ANNEX A**

### **LC-QTOF-MS analysis of the influent wastewater**

The wastewater sample was submitted to a solid-phase extraction (SPE) protocol prior to their analysis by Liquid Chromatography Quadrupole Time-of-flight Tandem Mass Spectrometry (LC-QTOF-MS/MS). Thus, 100 mL of the sample were passed through two 150 mg cartridges OASIS WCX and OASIS WAX (Waters, Milford, MA, USA) connected in series. The cartridges were previously conditioned following the manufacturer's specifications. After sample loading, the cartridges were dried under nitrogen stream for 20 minutes and eluted with 4 consecutive fractions consisting of 1) 10 mL of methanol, 2) 10 mL of methanol containing 5 % of ammonia, 3) 10 mL of methanol containing 2% of formic acid and 4) 10 mL of ethyl acetate. All these fractions were evaporated to dryness and reconstituted in 100 µL of methanol. The final extracts were injected (10 µL) into a LC-QTOF-MS 6520 system (Agilent Technologies, Santa Clara, USA). The chromatographic column was a Synergy Fusion-RP 100x2mm, 4µm (Phenomenex, Torrance, CA, USA) and the mobile phases consisted of ultrapure water (A) and methanol (B) both containing 0.1% formic acid. After the injection, the column was maintained at 95% A during 1 min, then, a linear gradient of 15 minutes was programmed from 95% A to 100% B (hold for 5 min) and the system was maintained at initial conditions again for other 10 min before the following injection. The QTOF-MS system worked in the "All Ions" acquisition mode using a collision energy of either 0 or 20 V (as to obtain the pseudomolecular ion and product ions), in both electrospray (ESI) positive and negative modes. Nitrogen was used as nebulizing (40 psi) and drying gas (300 °C, 5 L min<sup>-1</sup>) in the dual ESI source and also as collision gas in the MS/MS and All Ions experiments. The QTOF instrument was operated in the high resolution 4 GHz mode. This mode provides a full width at half-maximum (FWHM) resolution of ca. 10 600 at *m/z* 118.0862 and ca. 16 900 at *m/z* 922.0097. A reference calibration solution, supplied by Agilent, was continuously sprayed in the source during the chromatographic run, providing the required accuracy of mass assignments, according to the manufacturer instructions.

The MS data treatment was made with the MassHunter B.07.01 software using the algorithm "Find by Formula" with fragment confirmation against the Agilent Forensic Toxicology, Veterinary Drugs, Pesticides and Water Pollutants Libraries, which all together contain ca. 11,000 chemicals, of which

about 3,500 have MS/MS spectra. Tentatively identified compounds were reinjected in MS/MS mode at 10, 20 and 40 V collision energies for further confirmation. Blank samples of the whole analytical process were also processed and chemicals were only reported if they were detected in at least two replicate analysis of the sample and its signal was 5 times higher than the blank.

The identified compounds are shown in Table S1, classified in confirmatory levels, according to Schymanski et al., 2014. Only those compounds at a high enough confirmation level (level 2b or higher) are reported. The presence of twelve out of 20 analytes was confirmed through their comparison with reference standards (Level 1), 5 analytes were confirmed by matching their structure with different commercial libraries (Level 2a) and finally 3 compounds were tentatively identified by checking the possible fragmentation pattern (Level 2b).

Table S1. Summary of chemicals detected in the wastewater sample.

Compound detected	Level*	Fórmula	Rt (min)	ESI mode	Uses	CAS
Metformin	1	C4 H11 N5	1.8	+	Hypoglycemic	657-24-9
Paracetamol	1	C8 H9 N O2	3.5	+	Analgesic	103-90-2
Dibutylphthalate	1	C16 H22 O4	18.9	+	Plasticizer	84-74-2
Benzophenone 8	1	C14 H12 O4	16.4	+	UV filter	131-53-3
TCPP	1	C9 H18 Cl3 O4 P	17.2	+	Flame retardant	13674-84-5
Piperine	2a	C17 H19 N O3	17.7	+	Food additive	94-62-2
Methyl paraben	1	C8H8O3	14.6	-	Antimicrobial agent	99-76-3
Triclosan	1	C12H7Cl3O2	18.5	-	Antiseptic	3380-34-5
Netilmicin	2b	C21 H41 N5 O7	12.6	+	Antibiotic	56391-56-1
Irbesartan	1	C25 H28 N6 O	16.1	+	Antihypertensive	138402-11-6
Valsartan	1	C24H29N5O3	16.9	-	Antihypertensive	137862-53-4
Diclofenac	1	C14 H11 Cl2 N O2	18.1	+	Antiinflammatory	15307-86-5
Hippuric acid	2a	C9 H9 N O3	4.8	+	Bactericide	495-69-2
Fenofibric acid	2a	C17 H15 Cl O4	17.9	+	Antihyperlipidemic	42017-89-0
Acesulfame	1	C4H5NO4S	2.5	-	Sweetener	33665-90-6
4-Hydroxybenzoic acid	2a	C7H6O3	11.3	-	Chemical reagent / parabens metabolite	99-96-7
Chenodiol	2a	C24H40O4	19.0	-	Anticholesterolemic Ibuprofen (NSAID)	474-25-9
Carboxyibuprofen	2b	C13H16O4	14.8	-	metabolite	15935-54-3
Saccharin	1	C7H5NO3S	3.8	-	Sweetener	128-44-9
Canbisol	2b	C24 H38 O3	19.3	+	Syntetic cannabinoid	56689-43-1

\* Confirmation level according to Schymanski et al. (2014).

**Table S1.** Primer sequences and respective annealing temperature used in qPCR.

Gene	Genbank access number	Forward primer (5'-3')	Reverse primer (5'-3')	T <sub>annealing</sub> (°C)
RXR $\alpha$	NM_001161551	ATTCAATGGCATC TCCTG	GCGGCTTAATA TCCTCTG	60
PPAR $\gamma$	NM_131467	GGTTTCATTACGG CGTTCAC	TGGTTCACGTC ACTGGAGAA	60
SREBP1	NM_001105129.1	CAGAGGGTGGGC ATGCTGGC	ATGTGACGGTG GTGCCGCTG	60
FASn	XM_682295	ATCTGTTCTGTT CGATGGC	AGCATATCTCG GCTGACGTT	62
ACOX1	BC097101.1	GCACGGATGTGT GTACCGTGC	GCGTCCAGAGC CCCTTGACCT	62
C/EBP $\alpha$	NM_131885	AACGGAGCGAGC TTGACTT	AAATCATGCCC ATTAGCTGC	62
DGAT2	NM_001030196	TGGGGCTTTTTGT AACTTCG	TCTTCCTGGTG CACAGTCC	62
$\beta$ -actin	NM_181601.3	ACTGTATTGTCTG GTGGTAC	TACTCCTGCTT GCTAATCC	60

**Table S2.** Primers designed to amplify the HR+LBD of the NRs. Forward primers contain the recognition sequence of XbaI; Reverse primer contains the sequence for KpnI.

NR	Forward Primer (5'-3')	Reverse Primer (5'-3')
RXR $\alpha$	ATCGTCTAGACAGCGAGCCAA GGAACGC	AATTGGTACCTTATGTCATTTGG TGTGGAGCTT
PPAR $\gamma$	ATCGTCTAGACTGGCCGAGTTC TCCAGT	AATTGGTACCTTAGTACAGGTCC CGCATGA

**REFERENCES:**

Schymanski, E. L., Jeon, J., Gulde, R., Fenner, K., Ruff, M., Singer, H. P., Hollender, J., 2014. Identifying Small Molecules via High Resolution Mass Spectrometry: Communicating Confidence Environ. Sci. Technol. 48 (4), 2097–2098.  
<https://pubs.acs.org/doi/abs/10.1021/es5002105>.